Polymer Chemistry

ROYAL SOCIETY OF CHEMISTRY

COMMUNICATION

View Article Online
View Journal | View Issue

Open Access Article. Published on 05 luglio 2022. Downloaded on 30/06/2025 12:06:00.
This article is licensed under a Creative Commons Attribution-NonCommercial 3.0 Unported Licence.

Check for updates

Cite this: *Polym. Chem.*, 2022, **13**, 4086

Received 28th April 2022,
Accepted 19th May 2022

DOI: 10.1039/d2py00548d

rsc.li/polymers

Reinforcement of ultrahigh thermoresistant polybenzimidazole films by hard craters†

Jiabei Zhou, [a] Xianzhu Zhong, [a] Aniruddha Nag, [a,b] Yang Liu,[a] Kenji Takada [a] and Tatsuo Kaneko *[a]

Porous structures were formed in polybenzimidazole derivative films by a silica template method, followed by HF etching. As expected, the resulting ultrahigh thermoresistant films showed better elongation properties than did the non-porous films, with renewed strength and hardness. Microscopic analyses revealed that the pores were clearly formed, and craters with swollen edges and hardened surfaces were also observed.

Production of bioplastics from renewable biological resources is imperative for developing a sustainable society and achieving low-carbon technology.[1] One of the major research topics in this regard is the synthesis of highly heat-resistant bioplastics because carbon dioxide in the atmosphere can be immobilized in durable materials for a considerable amount of time. For instance, 3-amino-4-hydroxybenzoic acid produced by genetically modified *Escherichia coli* can be converted to polybenzimidazole and its copolymers, both of which have extremely high heat resistance. Despite having the highest thermal decomposition temperature on record, polybenzimidazole-*co*-polyamide (poly(DABA-*co*-ABA)) films are found to be brittle in nature due to their rigid chain structure. Numerous studies have been conducted to improve the flexibility of polybenzimidazole through molecular design,[2] inorganic composites,[3] and porous structure formation,[4] among others. Porous structure formation can influence the merits of lightweight, physical stability, and high resiliency, which has attracted the attention of researchers in the last few decades.[5] Luo and coworkers prepared porous PBI films using a phase separation process induced by water vapour. Chaudhari and coworkers prepared these films using the immersion precipitation method.[6] The effects of the porous structure on the mechanical properties of the films are rarely discussed in those reports, but the results reveal that the formation of porous structures improves the elongation rate of the material while degrading their mechanical properties. On the other hand, the silica (SiO_2) hard-template method, which is primarily used for water-absorbable materials such as hydrogels does not alter the components or chemical structure of the polymer, thus being a promising strategy for the processing of materials.[7] In our study, we discovered that high-performance polymer films are also water-absorbable plastics due to their polar structures.[8] Therefore, porous structures were cast in poly(DABA-*co*-ABA) films, and the hard-template method using SiO_2 nanoparticles was adopted to improve their stretchability and hardness (Fig. 1).

To form pores in poly(DABA-*co*-ABA), SiO_2 having a particle size of 300 nm was added to a mixed solution of poly(DABA-*co*-ABA) in trifluoroacetic acid (TFA)/methanesulfonic acid (MSA) and stirred until dissolution. Then, a PBI-SiO_2 composite film was produced by casting the mixed solution onto a glass substrate. The obtained film was etched with hydrofluoric acid (HF) to obtain a poly(DABA-*co*-ABA) porous film. The Fourier transform infrared (FT-IR) spectrum of SiO_2 showed a broad absorption band at 1000–1180 cm^{-1}, which was assigned to the Si–O–Si groups (Fig. S2†). As for the pristine poly(DABA-*co*-ABA), the characteristic bands at 1636, 1553, and 1284 cm^{-1} were assigned to the stretching vibration of the C=N, C=C, and C–N groups, respectively, and the broad absorption band at 3250–3450 cm^{-1} corresponded to N–H groups. A medium-strong peak was observed at 1000–1180 cm^{-1} in the spectrum

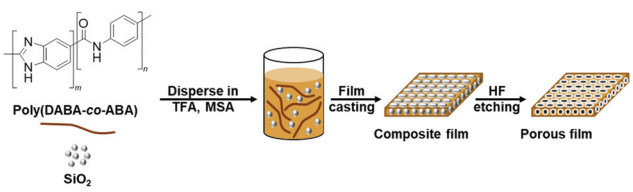

Fig. 1 Preparation of porous poly(DABA-*co*-ABA) films.

[a]*Graduate School of Advanced Science and Technology, Japan Advanced Institute of Science and Technology, 1-1 Asahidai, Nomi, Ishikawa, 923-1292, Japan. E-mail: kaneko@jaist.ac.jp*
[b]*School of Energy Science and Engineering, Vidyasirimedhi Institute of Science and Technology, Wangchan Valley 555 Moo 1 Payupnai, Wangchan, Rayong 21210, Thailand*

† Electronic supplementary information (ESI) available. See DOI: https://doi.org/10.1039/d2py00548d

This journal is © The Royal Society of Chemistry 2022

Open Access Article. Published on 05 luglio 2022. Downloaded on 30/06/2025 12:06:00.
This article is licensed under a Creative Commons Attribution-NonCommercial 3.0 Unported Licence.

of the composite poly(DABA-*co*-ABA), confirming that the SiO_2 nanoparticles were templated. After HF etching, the Si–O–Si absorption peak disappeared from the spectrum of the porous poly(DABA-*co*-ABA), indicating that the SiO_2 nanoparticles were completely removed and no change in the chemical structure occurred since the observed characteristic peaks of pristine poly(DABA-*co*-ABA). Based on these results, visual confirmation through scanning electron microscopy (SEM) was carried out to establish that pores were actually formed in the poly(DABA-*co*-ABA) film (Fig. 2). The pristine poly(DABA-*co*-ABA) film, as seen in Fig. 2a, was dense and homogenous with no pores on both the surface and the edge. As for the porous poly(DABA-*co*-ABA) films, nanoporous structures with a diameter of about 300 nm were observed on the surface and the edges after HF etching, corresponding to the size of the used SiO_2 nanoparticles (Fig. 2b and c).

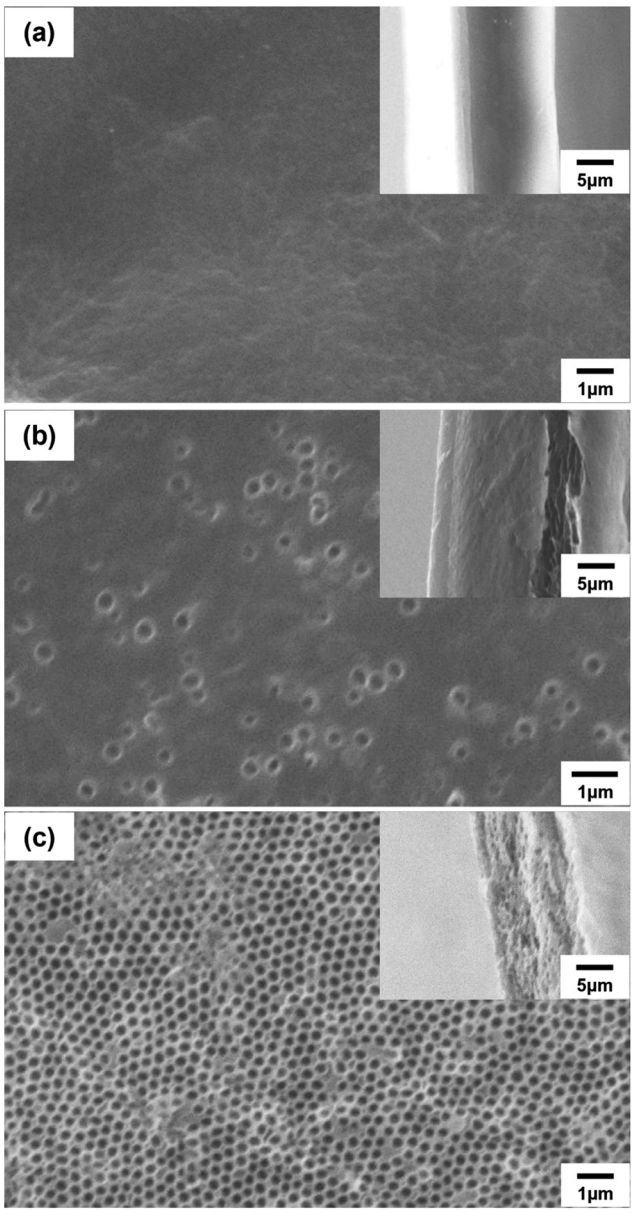

Fig. 2 SEM images of (a) pristine poly(DABA-*co*-ABA), (b) porous poly (DABA-*co*-ABA)-30%, and (c) porous poly(DABA-*co*-ABA)-50% film. SEM images of cross-section of films are inset.

PBI has high elastic properties because of its rigid backbone, numerous hydrogen bonds and strong intermolecular interactions. Furthermore, it is well-known that when pores are introduced into polymer films, the elongation ratio is improved, but the strength and hardness are significantly reduced.[9] On the other hand, after introducing pores into the poly(DABA-*co*-ABA) films, Young's modulus increased from 2.9 to 3.4 GPa for the film (including pore area for calculation) and from 2.9 to 8.4 GPa for matrix polymers (excluding pore area for calculation) (Table 1). Elongation at break increased from 2.6 to 12.7%, as expected. The strain energy density (toughness) increased from 0.7 MJ m^{-3} for pristine poly(DABA-*co*-ABA) film to 18.7 MJ m^{-3} for porous poly(DABA-*co*-ABA) film. In addition, an improved toughness was observed at the SiO_2 nanoparticles addition of 10 wt%, and the toughness improved as increasing the amount of SiO_2 nanoparticles (Fig. S3†). From these results, the introduction of porous structures by HF etching of SiO_2 nanoparticles forms a hard crater and shows higher strength than pristine poly(DABA-*co*-ABA) film. At the same manner, it also appears the effect of improving the elongation rate due to introducing the porous structures. These effects led to the synergistic improvement of the mechanical properties. As stated earlier, the pores usually compromise the mechanical properties, but the porous poly (DABA-*co*-ABA) film displayed an improvement in both toughness and stiffness (Young's modulus) as compared to those of the pristine poly(DABA-*co*-ABA) film. Regarding poly(DABA-*co*-ABA) without pores, there was no change in the mechanical properties before and after HF treatment (Fig. S4†). From this result, it was strongly suggested that the toughness improvement of porous poly(DABA-*co*-ABA) films was due to the introduction of the porous structures. Meanwhile, unlike the porous structures reported in other works, a rim of the white region was seen around each of the pores, circumscribing them (Fig. 2b and c). These unusual regions were investigated by a scanning probe microscope (SPM, SHIMADZU NANOA). These white rims around each pore appear brighter than the area apart from the pores, indicating that these rims areas (around the pores) are higher or elevated than the rest of the

Table 1 Mechanical properties of pristine poly(DABA-*co*-ABA) and porous poly(DABA-*co*-ABA)-50% films

Mechanical property	Pristine film	Porous film
Stress[a] (MPa)	47 ± 1	71 ± 3 (169 ± 6)
Strain[a] (%)	2.6 ± 0.1	12.7 ± 0.1 (12.7 ± 0.1)
Young's modulus[a] (GPa)	2.9 ± 0.1	3.4 ± 0.1 (8.4 ± 0.3)
Toughness[a] (MJ m^{-3})	0.7 ± 0.1	7.9 ± 0.1 (18.7 ± 0.3)
Elastic modulus[b] (MPa)	72	672 ± 36

[a] Properties of entire films including pore volume. The value in parentheses were the properties based on the polymer matrix which was calculated from excluding pore volume. [b] Calculated from the Johnson–Kendall–Roberts (JKR) model.

Open Access Article. Published on 05 luglio 2022. Downloaded on 30/06/2025 12:06:00.
This article is licensed under a Creative Commons Attribution-NonCommercial 3.0 Unported Licence.

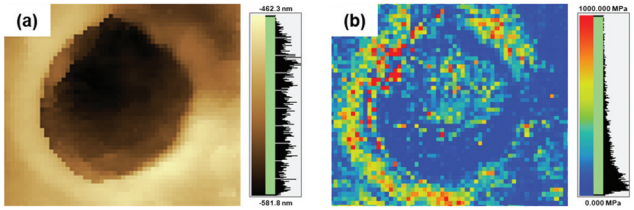

Fig. 3 SPM images of the (a) height and (b) elastic modulus of porous poly(DABA-*co*-ABA)-50% film.

area (Fig. 3a). Moreover, the elastic modulus of the white rim area (672 MPa), calculated from SPM force curve mode, is much higher than that of the area apart from the pore (72 MPa). With reference to the SPM images, it is evident that the elastic modulus of the white rim around the pore is higher than the rest of the area, thereby constituting an anomalistic behaviour.

The crystallinity and orientation of pristine and porous poly (DABA-*co*-ABA) were investigated by wide-angle X-ray diffraction (WAXD) to determine the causes of the improvements in mechanical properties (Fig. 4). The peak position (2θ) and *d*-spacing of pristine as well as porous poly(DABA-*co*-ABA) from WAXD were found to be 26.3 and 0.14 nm, respectively. However, the pristine poly(DABA-*co*-ABA) had a degree of orientation of 0.8 and a crystal size of 0.1 nm, while the porous poly (DABA-*co*-ABA) had a degree of orientation of 0 and a crystal size of 0.2 nm, implying that the formation of pores in poly (DABA-*co*-ABA), led to a decrease in its orientation and crystallinity, but an increase in crystal size. Furthermore, the degree of crystallinity for pristine and porous poly(DABA-*co*-ABA) were 7.8 and 4.9%, respectively. The decrease in the orientation and crystallinity possibly cause a reduction of modulus and strength, but the strength in elastic modulus of the rim areas brought a much greater effect on enhancing mechanical properties, as a result, the negative influence of decreased orientation and crystallinity was offset and a general increase in modulus and strength was manifested. This observation, along with the results of the SPM analysis demonstrates that pore formation improved the elongation ratio and mechanical properties of the entire poly(DABA-*co*-ABA) film.

The surface energy causes the poly(DABA-*co*-ABA) film covering the SiO_2 nanoparticles to form a crater-like shape in the holes formed by the SiO_2 nanoparticles removal. This formation may be attributed to the enhancement of intermolecular hydrogen bonds of poly(DABA-*co*-ABA) chains in the presence of HF

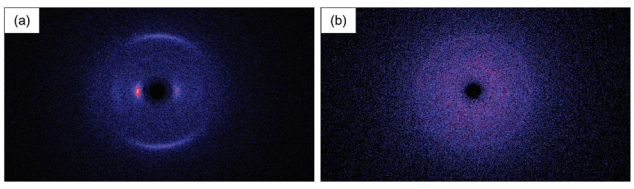

Fig. 4 WAXD images of the pores in (a) pristine poly(DABA-*co*-ABA) and (b) porous poly(DABA-*co*-ABA)-50% film.

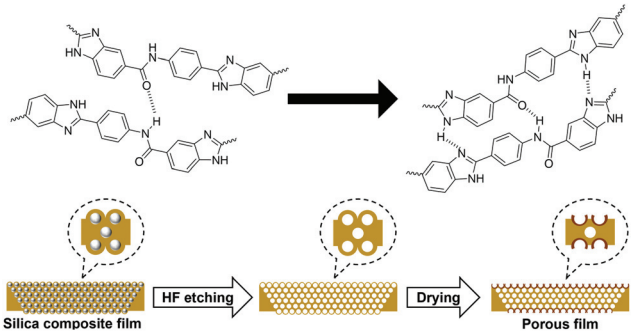

Fig. 5 The mechanism for the formation of hard craters in poly(DABA-*co*-ABA) film.

aqueous solution plasticizer, as well as the reduction of free energy due to the disappearance of SiO_2 nanoparticles (Fig. 5). In the case of using SiO_2 nanoparticles with a particle diameter of 20 nm, uniform pores were not observed due to aggregation of the SiO_2 nanoparticles (Fig. S5†). However, even in this case, where the particle size is not uniform, a white region around the pores was also observed as well, indicating the formation of "hard craters". This result indicated that it is effective to improve the mechanical properties by SiO_2 addition and HF etching into the polymer.

To summarise, poly(DABA-*co*-ABA) films with a porous structure were prepared by means of a hard-template method using SiO_2 nanoparticles. The craters formed on the films measured diametrically from 200 to 300 nm and the porosity of the films was adjusted by changing the volume of added SiO_2 nanoparticles during the preparation stage. The porous poly(DABA-*co*-ABA) films thus prepared, showed 4.9 fold higher elongation at break than the pristine ones, attributed to their porous structure. Surprisingly, Young's modulus was also found enhanced in porous poly(DABA-*co*-ABA) films. The porous structure increased the toughness of the pristine poly (DABA-*co*-ABA) film by 11 fold as whole materials (including pore volume) and by 27 fold in matrix polymers (excluding pore volume). SEM analyses revealed a white edge circumscribing each of the pores and SPM analyses attested the hardness of these edges. WAXD analyses revealed an increased crystal size of poly(DABA-*co*-ABA) films due to the formation of pores. The findings indicate that the hard craters formed on the film surface helped to reinforce the mechanical properties of the film. The porous poly(DABA-*co*-ABA) films were extremely thermoresistant and qualified for applications such as catalyst support, gas storage, proton exchange, and so on. Moreover, the hard-template method using SiO_2 nanoparticles followed with etching by HF aqueous solution would be beneficial for similar experimentation with films composed of water-absorbable polar polymers such as polyimides, polyamides, polyurethanes, and polyesters.

Conflicts of interest

There are no conflicts to declare.

This journal is © The Royal Society of Chemistry 2022

Open Access Article. Published on 05 luglio 2022. Downloaded on 30/06/2025 12:06:00.
This article is licensed under a Creative Commons Attribution-NonCommercial 3.0 Unported Licence.

Acknowledgements

This work has been financially supported by Japan Society for the Promotion of Science (JSPS) of Grant-in-Aid for Scientific Research (A) (22H00332), and Cross-ministerial Strategic Innovation Promotion Program (SIP2), "Smart-bio" (Bio-oriented Technology Research Advancement Institution, NARO, Japan). Moreover, authors would like to thank Shiho Moriguchi, Shogo Onomura of Shimadzu Techno-Research, INC. and Masato Hirade of SHIMADZU CORPORATION.

Notes and references

1 (*a*) Q. Xia, C. Chen, Y. Yao, J. Li, S. He, Y. Zhou, T. Li, X. Pan, Y. Yao and L. Hu, *Nat. Sustainability*, 2021, **4**, 627–635; (*b*) J. G. Rosenboom, R. Langer and G. Traverso, *Nat. Rev. Mater.*, 2022, **7**, 117–137.

2 (*a*) X. Tian, S. Wang, J. Li, F. Liu, X. Wang, H. Chen, D. Wang, H. Ni and Z. Wang, *Appl. Surf. Sci.*, 2019, **465**, 332–339; (*b*) X. Wang, W. Chen, X. Yan, T. Li, X. Wu, Y. Zhang, F. Zhang, B. Pang and G. He, *J. Power Sources*, 2020, **451**, 227813.

3 (*a*) Y. Wang, L. Chen, J. Yu, J. Zhu, Z. Shi and Z. Hu, *RSC Adv.*, 2013, **3**, 12255–12266; (*b*) J. Kim, K. Kim, T. Ko, J. Han and J. Lee, *Int. J. Hydrogen Energy*, 2021, **46**, 12254–12262.

4 (*a*) L. Zeng, T. S. Zhao, L. An, G. Zhao and X. H. Yan, *Energy Environ. Sci.*, 2015, **8**, 2768–2774; (*b*) K. Geng, H. Tang, Q. Ju, H. Qian and N. Li, *J. Membr. Sci.*, 2021, **620**, 118981.

5 (*a*) X. Cui, C. Zhang, S. Araby, R. Cai, G. Kalimuldina, Z. Yang and Q. Meng, *J. Ind. Eng. Chem.*, 2022, **105**, 549–562; (*b*) P. S. Pálvölgyi, D. Sebők, I. Szenti, E. Bozo, H. Ervasti, O. Pitkänen, J. Hannu, H. Jantunen, M. E. Leinonen, S. Myllymäki, A. Kukovecz and K. Kordas, *Nano Res.*, 2021, **14**, 1450–1456; (*c*) B. Sarkar, X. Li, E. Quenneville, L. Carignan, K. Wu and F. Cicoira, *J. Mater. Chem. C*, 2021, **9**, 16558–16565.

6 (*a*) T. Luo, B. Dreusicke and M. Wessling, *J. Membr. Sci.*, 2018, **556**, 164–177; (*b*) H. D. Chaudhari, R. Illathvalappil, S. Kurungot and U. K. Kharul, *J. Membr. Sci.*, 2018, **564**, 211–217.

7 (*a*) W. Jiang, Y. Zhu, G. Zhu, Z. Zhang, X. Chen and W. Yao, *J. Mater. Chem. A*, 2017, **5**, 5661–5679; (*b*) E. H. Borai, M. G. Hamed, A. M. El-kamash, T. Siyam and G. O. EI-Sayed, *J. Colloid Interface Sci.*, 2015, **456**, 228–240.

8 (*a*) A. Nag, M. A. Ali, H. Kawaguchi, S. Saito, Y. Kawasaki, S. Miyazaki, H. Kawamoto, D. T. N. Adi, K. Yoshihara, S. Masuo, Y. Katsuyama, A. Kondo, C. Ogino, N. Takaya, T. Kaneko and Y. Ohnishi, *Adv. Sustainable Syst.*, 2021, **5**, 2000193; (*b*) X. Zhong, A. Nag, J. Zhou, K. Takada, F. A. A. Yusof, T. Mitsumata, K. Oqmhula, K. Hongo, R. Maezono and T. Kaneko, *RSC Adv.*, 2022, **12**, 11885–11895.

9 (*a*) K. Taki, K. Hosokawa, S. Takagi, H. Mabuchi and M. Ohshima, *Macromolecules*, 2013, **46**, 2275–2281; (*b*) L. Jheng, W. J. Chang, S. L. Hsu and P. Cheng, *J. Power Sources*, 2016, **323**, 57–66; (*c*) X. Che, H. Zhao, X. Ren, D. Zhang, H. Wei, J. Liu, X. Zhang and J. Yang, *J. Membr. Sci.*, 2020, **611**, 118359.